

## External Protons Enhance the Activity of the Hyperpolarization-activated K Channels in Guard Cell Protoplasts of *Vicia faba*

N. Ilan<sup>1</sup>, A. Schwartz<sup>1</sup>, N. Moran<sup>2</sup>

<sup>1</sup>Department of Botany, Faculty of Agriculture, the Hebrew University of Jerusalem

<sup>2</sup>Department of Neurobiology, Weizmann Institute of Science, Rehovot 76100 Israel

Received: 26 April 1996/Revised: 29 June 1996

**Abstract.** Hyperpolarization-activated K channels ( $K_H$  channels) in the plasmalemma of guard cells operate at apoplastic pH range of 5 to over 7. Using patch clamp in a whole-cell mode, we characterized the effect of varying the external pH between 4.4–8.1 on the activity of the  $K_H$  channels in isolated guard cell protoplasts from *Vicia faba* leaves.

Acidification from pH 5.5 to 4.4 increased the macroscopic conductance of the  $K_H$  channels by 30–150% while alkalization from pH 5.5 to 8.1 decreased it only by roughly 15%. The voltage-independent maximum cell conductance, increased by ~60% between pH 8.1 and 4.4 with an apparent  $pK_a$  of 5.3, most likely owing to the increased availability of channels. Voltage-dependent gating was affected only between pH 5.5 and 4.4. Acidification in this range shifted the voltage-dependent open probability by over 10 mV. We interpret this shift as an increase of the electrical field sensed by the gating subunits caused by the protonation of external negative surface charges. Within the framework of a surface charge model the mean spacing of these charges was ~30 Å and their apparent dissociation constant was  $10^{-4.6}$ . The overall voltage sensitivity of gating was not altered by pH changes. In a subgroup of protoplasts analyzed within the framework of a Closed-Closed-Open model, the effect of protons on gating was limited to shifting of the voltage-dependence of all four transition rate constants.

**Key words:** Stomata — Plant K-channel — Guard cell protoplast — Surface charge — pH effect — Channel gating model — Patch clamp

## Introduction

The hyperpolarization-activated K ( $K_H$ ) channels (termed also  $K_{in}$  channels), first described in broad bean (*Vicia faba*) guard cells (Schroeder, Raschke & Neher, 1987), exist in all higher plant cells examined so far, including barley aleurone cells, pulvini motor cells, mesophyll cells and root hairs cells (reviewed in Schroeder, Ward & Gassman, 1994). In the guard cells, which swell and shrink controlling leaf gas exchange, the  $K_H$  channels serve as the influx pathway for  $K^+$  during the swelling phase.  $K^+$  influx is powered by the activity of the proton pump, which hyperpolarizes the membrane and simultaneously acidifies the extracellular milieu (the apoplast; Raschke & Humble, 1973; Spanswick, 1981; Zeiger, 1983; Assmann, Simoncini & Schroeder, 1985; Shimazaki, Iino & Zeiger, 1986). Due to the proton pump action, the physiological apoplastic pH in closing and opening stomata varies between 7.2 and 5.1, respectively, as documented using fluorescence methods and  $H^+$ -sensitive electrodes (Edwards, Smith & Bowling, 1988). Similar variation of apoplastic pH was determined also in another type of motor cells, pulvinar extensor cells, with  $H^+$ -sensitive electrodes (Lee & Satter, 1989; Starrach & Mayer, 1989). In both motor cell types, the activity phase of the  $K_H$  channel appears to coincide with the lowest values of the apoplastic pH, as deduced from the observed simultaneous variations in the apoplastic  $K^+$  and  $H^+$  concentrations (guard cells: Bowling, 1987; Edwards et al., 1988; pulvinar cells: Lee & Satter, 1989; Lowen & Satter, 1989; Starrach & Mayer, 1989). This is intriguing in view of the commonly observed block of various K channels by external protons, including the recently described proton block of the depolarization-dependent K ( $K_D$ ) channel coexisting with the  $K_H$  channel in the guard cell plasma membrane

(Ilan, Schwartz & Moran, 1994a, and refs. therein). In fact,  $K^+$  influx (most probably through the ubiquitous  $K_H$  channels) occurs simultaneously with apoplast acidification also in expanding cells in the growing tissues of the plant (e.g., Marrè et al., 1974; Blum et al., 1992 and refs. therein).

While this phenomenon appears to be a general feature of plant physiology, very little is presently known about the interaction of the  $K_H$  channel with protons. The biochemical and biophysical characterization of the  $K_H$  channel, including proton effects, is particularly important now with the increasing number of new clones of this channel (Anderson et al., 1992; Sentenac et al., 1992; Muller-Rober et al., 1995; Ketchum & Slayman, 1996). A detailed description of the kinetic behavior of native plant  $K_H$  channels in protoplasts may serve as the basis for comparisons with the various cloned and/or mutated variants of this channel. Such comparisons are instrumental in gaining insight into the function-structure relationship of the various parts of the channel molecule responsible for gating (*see*, for example, Sigworth, 1995). So far, there are only a few descriptions of gating of *cloned*  $K_H$  channels (Hoshi, 1995; Muller-Rober et al., 1995; Hedrich et al., 1995; Véry et al., 1995), and even less information on gating of the *native*  $K_H$  channels (Blatt, 1992; Fairley-Grenot & Assmann, 1993; Schroeder, 1995). Moreover, the few reports on the effects of external protons on the cloned  $K_H$  channels (Hoshi, 1995; Muller-Rober et al., 1995; Hedrich et al., 1995; Véry et al., 1995) have been matched, so far, by only one detailed description of the effects of external protons on the native  $K_H$  channel in an *intact* guard cell of *Vicia faba* (Blatt, 1992).

The present study extends the characterization of the native plant  $K_H$  channel by describing its interaction with external protons (pH between 4.4–8.1) in *protoplasts* of *V. faba* guard cells. This interaction was resolved into voltage-dependent and independent components and a mathematical model was applied to describe the voltage-dependent gating of the  $K_H$  channel. In about half of the examined cells, the description of gating, based on the macroscopic kinetics of the  $K_H$  channels, required a minimum of three states: Closed<sub>1</sub>-Closed<sub>2</sub>-Open. Therefore, we used the framework of the three state model and described the gating of these channels and the effect of protons on it in terms of the Eyring rate theory, i.e., in terms of the rates of transitions between their conformational states. The effect of protons on gating consisted of a positive shift in the voltage-dependence of the transition rates, which we interpret as an increase in the electrical field in the membrane, due to the screening and titration of the external negative surface charges. The additional, voltage-independent effect of external protons consisted of an increased  $K_H$  channel availability.

Preliminary reports appeared in an abstract form (Ilan, Schwartz & Moran, 1994b, 1996).

## Materials and Methods

### EXPERIMENTAL METHODS

#### *Plant Material*

The procedure for growing *Vicia faba* plants and the enzymatic isolation of guard cell protoplasts is described by Ilan et al. (1994a).

#### *Electrophysiology*

The patch-clamp technique is described in detail by Hamill et al. (1981) and our application to *V. faba* guard cell protoplasts is described in detail by Ilan et al. (1994a). Briefly, a drop of the protoplast suspension was added to about 200  $\mu$ l of the recording solution, the protoplasts were allowed to settle and stick to the glass bottom of the recording chamber and then washed with about 2–3 ml of the recording solution. The patch pipette was then brought into contact with the protoplast and a “whole cell” configuration was attained through rupturing within the pipette rim by gentle suction.

All experiments were performed in a voltage-clamp mode, using the Axopatch C-1 amplifier (Axon Instruments, Foster City, CA), and were under computer control, using a software-hardware system from Axon Instruments (pCLAMP program package and the TL-1-125 Lab-master DMA A/D and D/A peripherals).

Membrane potential was controlled according to a preprogrammed schedule, and whole-cell membrane was filtered at 100–200 Hz (–3db, 4-pole Bessel filter), sampled at 400–1000 Hz and stored for further analysis. The error in voltage-clamping of the whole cell membrane, largely due to the access resistance,  $R_a$ , of the patch pipette was compensated at about 70% by analog circuitry of the Axopatch amplifier. These  $R_a$  values were about  $30 \pm 8$  M $\Omega$  (mean  $\pm$  SD,  $n = 27$ ). The resistance of the cells in the “whole-cell” configuration at rest was about  $4 \pm 2$  G $\Omega$  (mean  $\pm$  SD,  $n = 27$ ; determined from “leak” current, *see* below) and at peak activity it was  $160 \pm 12$  M $\Omega$  (mean  $\pm$  SD,  $n = 4$ ; based on  $G_k$  at –217 mV at pH 4.4). To enable comparison with other reports, these values may be normalized to the mean protoplast surface area of 865  $\mu$ m<sup>2</sup> (Ilan et al., 1994a). The measured membrane potential was corrected for liquid-junction potential determined separately using the experimental solutions and 3 M KCl-filled agar bridges (–17 mV; Neher, 1992).

#### *Solutions*

The intracellular solution in the patch pipette contained (in mM): 100 glutamate, 105  $K^+$ , 6  $Mg^{2+}$ , 4  $Cl^-$ , 0.2 BAPTA (estimated free  $[Ca^{2+}]_i < 10^{-7}$  M), 4 ATP, 20 HEPES, pH 7.2, and mannitol, to final osmolarity of 520 mOsm. Due to the effectively infinite increase of the cytoplasm volume in the whole-cell configuration and to the fast equilibration of small solutes in this combined pipette-cell compartment (Marty & Neher, 1993), the interior of the cell is “clamped” at pH 7.2, and the pH changes affect only the external cell surface. The control bath solutions contained (in mM): 11  $K^+$ , 1  $Ca^{2+}$ , 2  $Mg^{2+}$ , 6  $Cl^-$ , 10 glutamate, 10 MES and 0.25–0.5 n-methylglucamine (NMG), pH 5.5. Bath solution for pH 4.4 included (in mM): 100 MES, rather than 10 or 7 glutamate and 10 MES (we did not observe any differences between the two subgroups). For pH 5 it included 20 mM MES and for pH 8 it included 10 mM HEPES, rather than MES; and, in addition, 7.5 mM of NMG. Final

osmolality of all bath solutions was adjusted with mannitol to 480 mOsm. BAPTA- $K_4$  was from Molecular Probes, Eugene, OR. Mannitol was from Merck. All other chemicals were from Sigma. In all the following calculations ion “concentrations” indicate, in fact, activities, calculated using coefficients from Robinson and Stokes (1965).

## THEORETICAL CONSIDERATIONS

The methods of analysis used here were already applied to characterize the effects of protons on the Depolarization-dependent  $K$  ( $K_D$ ) channels (Ilan et al., 1994a). Nevertheless, the equations, their descriptions and definitions have been repeated here for the sake of the readers' convenience, with only a few modifications.

### Initial Data Reduction

First, we obtained the whole-cell  $I$ - $E_m$  (current-voltage) relationships. Due to the delay in channel activation, the time-independent, “leak,” current could be determined at the beginning of a hyperpolarizing step from the resting potential. The steady-state  $K_H$  channel current values,  $I$ , were obtained by subtracting this leak current from the current measured at the end of a 2.5 sec voltage pulse. Then, the steady-state  $G_K$  (chord conductance) at various  $E_M$  was extracted using Eq. 1:

$$G_K = I/(E_M - E_{rev}), \quad (1)$$

where  $E_{rev}$  is the reversal potential (Hodgkin & Huxley, 1952) of this current.

When the  $K_H$  channels were opened by a hyperpolarizing pulse, the instantaneous  $I$ - $E_m$  relationship was linear over the examined  $E_M$  range, which justifies the use of Eq. 1 for the calculation of real  $G_K$ . This linearity of the open channel  $I$ - $E_M$ , even beyond  $E_{rev}$ , supports the findings that the hyperpolarization-induced activation of the plant inward rectifier channel is due to an intrinsic gating mechanism (Hedrich et al., 1995; Hoshi, 1995; Schroeder, 1995), and not to the removal of an intracellular  $Mg^{2+}$  block as in the animal inward rectifier.

In addition, we described the kinetics of current activation and of current deactivation first in terms of  $t_{1/2}$ s (half-activation times) and finally in terms of  $\tau$ s (time constants) vs.  $E_M$ . We obtained these  $\tau$ s by fitting current relaxations (corrected for filter delay of 2–2.5 msec<sup>1</sup>) with two exponential terms. In about half of the cells at least three exponentials were required to describe the activation time courses of the currents, while two exponentials sufficed in the other cases. In the experiments described here, the analysis of channel kinetics (CCO modeling, *see below*) was limited to the subset of cells with two-exponential activation kinetics, that contained data points at a sufficiently large range of voltages (Ilan et al., 1994a). For the steady-state analyses both types of cells were pooled. The steady-state voltage dependence of these two groups (analyzed at the control pH of 5.5, within the framework of the two-state model) was identical.

### Modeling—An Overview

We used the “macroscopic” steady-state whole cell-data for all of our analyses, examining separately the effect of pH on voltage-independent, and the voltage-dependent properties. In the modeling of the voltage-dependent  $K_H$  channel gating, we combined the informa-

tion about these voltage-dependent *steady-state* properties with the information about the voltage-dependent *kinetics* of activation and deactivation. It is important to emphasize that due to the scatter of the pooled data, we did not attempt to compare and choose among different models (except when fitting the activation and deactivation time courses). We did, however, use several widely accepted general minimal models (*see below*) and based on these, we extracted estimates of the models' parameters. Our only claim is that these parameters are unique.

### Boltzmann Distribution

The voltage dependence of the steady-state  $G_K$  resides in the probability for the  $K_H$  channel to be open,  $P_o$ :

$$G_K = G_{max} \cdot P_o, \quad (2)$$

where  $G_{max}$  is the voltage-independent maximum value of  $G_K$ .

Assuming an equilibrium distribution of the  $K_H$  channels between a Closed and an Open state, and replacing the voltage-dependent  $P_o$  with a simple Boltzmann equation:

$$P_o = 1/(1 + e^{-zF(E_M - E_{1/2})/RT}), \quad (3)$$

where  $E_{1/2}$  is the half-activation voltage,  $z$  is the number of effective charges transferred upon activation,  $R$  is the universal gas constant,  $F$  is the Faraday constant and  $T$  is the absolute temperature, we fitted the individual steady-state  $G_K - E_M$  relationships for each cell and pH with the combined equation:

$$G_K = G_{max}/(1 + e^{-zF(E_M - E_{1/2})/RT}) \quad (4)$$

The resulting values of  $G_{max}$  and  $E_{1/2}$  were used in subsequent analyses.

### Henderson-Hasselbalch Relationship for $G_{max}$

By definition,  $G_{max}$  is voltage-independent. We assumed that  $G_{max}$  increases with acidification as does the fraction of the protonated form of the  $K_H$  channel, and that only one site undergoes protonation. Therefore, we fitted the mean  $G_{max}$ -pH data determined between pH 8.1 and 4.4 with the Henderson-Hasselbalch relationship:

$$G_{max} = G'/(1 + 10^{pH - pK_a}) + G_{basal} \quad (5)$$

where  $G'$  is the maximum conductance with full protonation,  $G_{basal}$  is the conductance in absence of protonation and  $pK_a$  is the pH at which half of the sites are protonated.  $G_{max}$  is composed of  $N$ , the number of available channels in the membrane, and  $\gamma_s$ , the single channel conductance:

$$G_{max} = N \cdot \gamma_s, \quad (6)$$

and, furthermore,

$$N = N' \cdot f_a, \quad (7)$$

where  $N'$  is the total number of channel molecules in the membrane and  $f_a$  is the fraction of channels that can respond (by conformational changes) to alterations of the electric field in the membrane. This responsivity, in turn, may be determined by modulatory effects, such as phosphorylation, methylation or protonation of the channel protein itself or an adjacent molecule. In view of the fast reversibility of pH effects on  $G_{max}$ , it is unlikely that changes in  $G_{max}$  reflect changes in

<sup>1</sup> Based on the 4-pole Bessel filter specifications, as in “Active filter products design and selection guide”; Frequency Devices, Haverhill, MA.

$N'$ . Rather, changes in  $G_{\max}$  ought to be sought either in  $\gamma_s$  or in  $f_a$  (or both).

### Surface Charge

$E_{1/2}$  characterizes the voltage-dependent gating. We assumed that the shift of  $E_{1/2}$  ( $\Delta E_{1/2}$ ) with acidification results from the screening and filtration of negative charges at the external surface of the membrane in the vicinity of the  $K_H$  channel (Gilbert & Ehrenstein, 1969, 1970), and fitted the pooled  $\Delta E_{1/2}$ -pH relationship with the Grahame equation (Grahame, 1947):

$$\sigma^2 = G^{-2} \sum_i c_i (e^{-z_i F(B - \Delta E_{1/2})/RT} - 1) \quad (8)$$

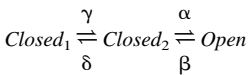
modified to include proton binding (Gilbert & Ehrenstein, 1969, 1970):

$$\sigma^2 = \sigma_t^2 \left( 1 + \frac{[H^+]_o}{K_{sc}} e^{-F(B - \Delta E_{1/2})/RT} \right)^{-2}, \quad (9)$$

where  $\sigma$  is the free negative surface charge density,  $\sigma_t$  is the total density of the titratable negative charges,  $c_i$  are the concentrations of various ions in the medium,  $z_i$  are their respective valencies,  $K_{sc}$  is the dissociation constant of the protons from the negative surface charges,  $[H^+]_o$  is the proton concentration in the bulk solution,  $G$  is a constant equal to  $264 \text{ (}\AA/\text{electronic charge)} \cdot (\text{mole/liter})^{1/2}$  at  $23^\circ\text{C}$ , and  $B$  is the surface potential at the pH (5.5) at which the shift of  $E_{1/2}$  is defined as 0 mV. The actual parameters fitted were:  $d_i$  ( $=\sigma_t^{-0.5}$ ),  $pK_{sc}$  ( $=-\log(K_{sc})$ ) and  $B$ .

### The CCO Model

According to this model, the  $K_H$  channel undergoes the following transitions:



where  $\alpha$ ,  $\beta$ ,  $\gamma$ ,  $\delta$  denote the rate constants of transitions between the neighboring states.

We hypothesized that these rate constants are exponential functions of membrane potential (Hodgkin & Huxley, 1952; Ehrenstein et al., 1974):

$$\begin{aligned} \alpha &= B_2 e^{z_\alpha(E_M - E_2)F/RT}, \\ \beta &= B_2 e^{-z_\beta(E_M - E_2)F/RT}, \\ \gamma &= B_1 e^{z_\gamma(E_M - E_1)F/RT}, \\ \delta &= B_1 e^{-z_\delta(E_M - E_1)F/RT}, \end{aligned} \quad (10)$$

where  $E_M$  is the membrane potential,  $z_\gamma$  and  $z_\delta$  are the effective charges moved (number of elementary charges  $\times$  distance of movement) in the processes represented by rate constants  $\gamma$  and  $\delta$ , respectively,  $z_\alpha$  and  $z_\beta$  are the effective charges moved in the processes represented by  $\alpha$  and  $\beta$ ,  $E_1$  and  $E_2$  are membrane potentials at which the rates of the transitions in opposite directions between the neighboring states ( $C_1 \leftrightarrow C_2$  and  $C_2 \leftrightarrow O$ , respectively) are equal and  $B_1$  and  $B_2$  are the values of these rates at  $E_1$  or  $E_2$ , respectively. In a three state model, the time constants ( $\tau_s$ ) of current relaxations upon step changes of membrane potential, are complicated combinations of the transition rate constants (Huang, Moran & Ehrenstein, 1984):

$$\tau_{1,2} = \frac{2}{\alpha + \beta + \gamma + \delta \pm \sqrt{(\alpha + \beta + \gamma + \delta)^2 - 4(\alpha\gamma + \beta\gamma + \beta\delta)}} \quad (11)$$

In steady state conditions, the probability  $P_o$  for a three-state channel to be in an open (conducting) state is given by:

$$P_o = \frac{1}{1 + \beta/\alpha(1 + \delta/\gamma)} \quad (12)$$

or, with the ratios  $\beta/\alpha$  and  $\delta/\gamma$  replaced by two Boltzmann distributions governing the population of the three states (Behrens et al., 1989):

$$P_o = \frac{1}{1 + e^{-z_2 F(E_M - E_2)/RT} (1 + e^{-z_1 F(E_M - E_1)/RT})} \quad (13)$$

where  $z_1$  and  $z_2$  are the effective charges moved upon transitions  $C_1 \leftrightarrow C_2$  and  $C_2 \leftrightarrow O$ , i.e., the respective sums (in pairs) of  $z_\gamma$  and  $z_\delta$ , and of  $z_\alpha$  and  $z_\beta$ .

In fitting the steady-state  $P_o - E_M$  relationship with the CCO model (Eq. 13), we used  $G_K/G_{\max}$  as a measure of  $P_o$  (Eq. 2), where  $G_{\max}$  is the previously determined voltage-independent scaling factor of  $G_K$  (Eq. 4).<sup>2</sup>

Thus, within the framework of the three-state model, eight parameters and a scaling factor are required for the quantitative description of both the steady-state conductance and the conductance relaxation kinetics, as a function of membrane potential. These parameters can be extracted by a simultaneous fit of Eqs. 10–13, i.e.,  $\tau_1$ ,  $\tau_2$  and  $P_o$  vs.  $E_M$ , to the experimental data.

### Details of Analysis and Fitting

Nernst potentials were calculated from ion concentrations using activity coefficients from Appendices 8.9 and 9.10 from Robinson and Stokes (1965). Initial data reduction was performed with the pCLAMP software (Axon Instruments). In addition to analyses of macroscopic whole-cell currents, we used “pstat” ver. 6.02, to analyze single-channel bursts, (i) estimating the optimum interburst interval, (ii) using this value to obtain the distribution of burst durations, and (iii) fitting this distribution with one exponential to yield the mean burst duration. Mean  $\pm$  SD were used to indicate range of variability of various values. However, when comparison between means was intended,  $\pm$ SEM was used. The reversal potential was obtained as the zero-current intercept of a linear regression to instantaneous “tail”-current-voltage data points, and its asymmetrical lower and upper 95%-confidence limits were calculated by inverse regression (Sokal & Rohlf, 1981). Estimated parameters were given with their Estimated Errors (EE) or 95%-confidence limits, as indicated. Unless otherwise indicated,  $n$  signifies the number of points used for the fit. Outliers (points deviating from the mean by  $>2.5$  SD) were not included in the fit.

When fitting data with models, several starting guesses for the parameters were tried, to avoid “entrapment” in a local minimum. Data pooled from different experiments were fitted without averaging, but they are presented in the figures as means  $\pm$  SEM, for clarity. The weighing factor used in the fit of  $G_{\max}$  and  $E_{1/2}$  vs. pH was the inverse of the standard deviation calculated separately at each value of pH. This was based on the assumption that the data scatter need not be necessarily the same in the different conditions. When fitting the  $\tau_s$

<sup>2</sup> The steady-state  $P_o - E_M$  relationships of a two-state and a three-state channel are almost indistinguishable (Behrens et al., 1989; Ilan et al., 1994a) and both relationships yield the same  $G_{\max}$  value.

and  $P_o$  vs.  $E_M$  with the CCO model, the weighing factor was the inverse of the mean of each of the four groups to bring the calculated errors to a similar range of values:  $P_o$ ,  $\tau_1$  of activation combined with  $\tau_1$  of deactivation,  $\tau_2$  of activation,  $\tau_2$  of deactivation. To evaluate goodness of fit, we calculated  $R' = 1 - S_{res}/S_{tot}$ , where  $S_{res}$  is the sum of squared vertical deviations of data from the model predictions, and  $S_{tot}$  is the sum of squared vertical deviations of data points from the mean.  $R' = 1$  means perfect fit to the model,  $R' = 0$  means that the model is no better than a straight horizontal line drawn through the mean. The programs and procedures used for fitting were detailed by Ilan et al. (1994a).

Results

PROTON ENHANCEMENT OF THE MACROSCOPIC  $K_H$  CHANNEL CURRENTS AND CONDUCTANCE

Hyperpolarization of whole-cell membrane below  $-100$  mV elicited inward currents, whose magnitude was proportional to the amplitude of the hyperpolarizing step (Fig. 1). As shown by others (Schroeder, Raschke &

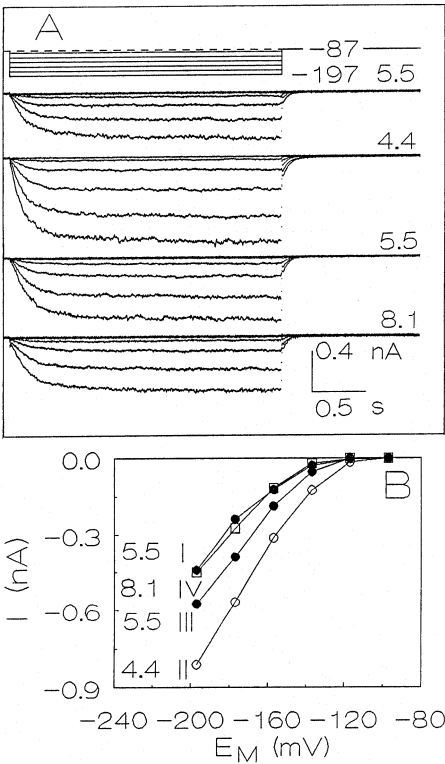


**Fig. 1.**  $K_H$  channel currents increase reversibly with acidification. (A) Traces (superimposed) of whole-cell currents from a single cell elicited by square voltage pulses from a holding potential of  $-87$  to  $-197$  mV,  $-177$ , mV, etc. (top panel) at the indicated external pH values (numbers at right). Interpulse-interval was 13 sec. (B) Steady-state net current-voltage ( $I$ - $E_M$ ) relationships (symbols, interconnected by lines) of currents in A at various indicated external pH values. Roman numerals indicate order of solution changes.

Neher, 1987; Schroeder, 1988; Fairley-Grenot & Assmann, 1992; Blatt, 1992; *see also* reviews by Hedrich & Schroeder, 1989, and Schroeder et al., 1994), these currents are carried through the hyperpolarization-activated K ( $K_H$ ) channels (corresponding to the  $K_m$  of Schroeder,

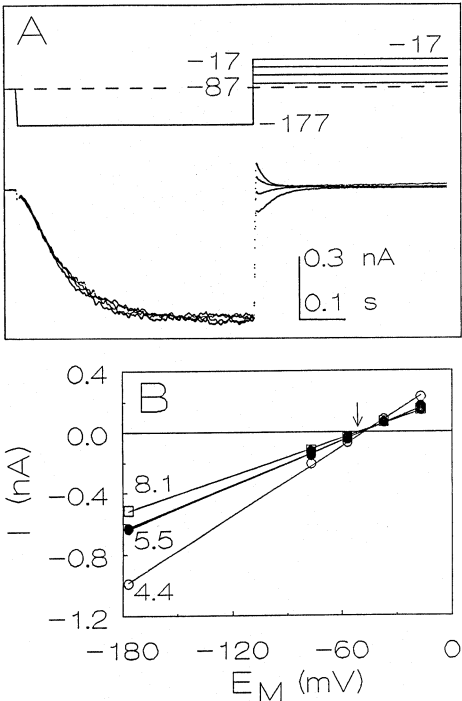


**Fig. 2.** External pH does not affect the reversal potential. (A) Two-pulse voltage protocol (top) elicited whole-cell membrane currents (superimposed, bottom). Note the change of direction of the ‘tail’ currents. Numbers indicate membrane potentials. Interpulse-interval was 13 sec. (B) Instantaneous  $I$ - $E_M$  relationships of the ‘tail’ currents of Fig. 2A (symbols). Lines: linear regressions to the data points. Note the linearity of these relationships. In this particular cell,  $G_K$  (the chord conductance,  $\pm$ SEM) changed from  $4.1 \pm 0.1$  nS at pH 8.1 ( $\square$ ), through  $5 \pm 0.1$  nS at pH 5.5 ( $\bullet$ ), to  $7.6 \pm 0.1$  nS at pH 4.4 ( $\circ$ ). The respective reversal potentials (and their 95% fiducial limits; *see* Materials and Methods) were:  $-51.5$  mV (between  $-41.4$  and  $-61.3$  mV),  $-49.5$  mV (between  $-44.3$  and  $-54.5$  mV) and  $-48.3$  mV (between  $-43.6$  and  $-52.9$  mV), respectively. Arrow indicates the Nernst potential for  $K^+$ .

**Table 1.** Average best-fit parameters of the Boltzman equation (Eq. 4) fitted to  $G_K$ - $E_M$  relationships at various pH values

Parameters	$G_{max}$ (nS $\pm$ SEM)	$E_{1/2}$ (mV $\pm$ SEM)	$z$ ( $\pm$ SEM)
pH			
4.4 ( $n = 13$ )	$6.60 \pm 0.40$	$-145.8 \pm 2.5$	$1.50 \pm 0.07$
5.0 ( $n = 5$ )	$6.54 \pm 0.35$	$-147.7 \pm 3.5$	$1.49 \pm 0.05$
5.5 ( $n = 33$ )	$5.30 \pm 0.05$	$-157.1 \pm 1.4$	$1.53 \pm 0.02$
8.1 ( $n = 12$ )	$4.25 \pm 0.25$	$-156.7 \pm 2.4$	$1.52 \pm 0.07$

The parameters were determined for each cell at each pH separately.  $n$  is the number of cells.

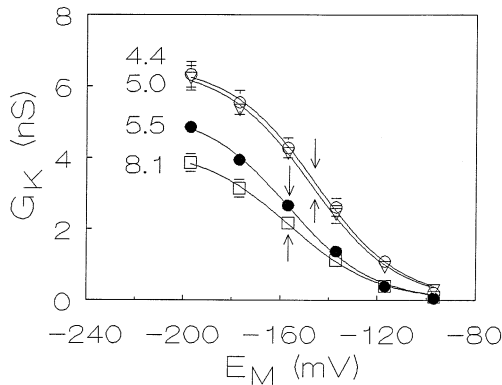


**Fig. 3.** Macroscopic  $K_H$  conductance increases with acidification. Average chord conductance,  $G_K$  (symbols,  $\pm$ SEM), from  $n$  cells, at the indicated pH values: 4.4 ( $\circ$ ,  $n = 13$ ), 5.0 ( $\nabla$ ,  $n = 5$ ), 5.5 ( $\bullet$ ,  $n = 33$ ), 8.1 ( $\square$ ,  $n = 12$ ). Lines: calculated from the simple Boltzmann equation (Eq. 4, Materials and Methods) using the averaged best-fit parameters determined at each pH for each cell separately, as listed in Table 1. Arrows indicate the values of mid-activation potential,  $E_{1/2}$  (Eq. 3).

1988). The lower the pH of the external medium, the larger were the hyperpolarization-activated inward currents. This effect was largely reversible (Fig. 1). The reversal potential ( $E_{rev}$ , Hodgkin & Huxley, 1952) of these currents at pH 5.5 was  $-52.0 \pm 3.5$  mV (mean  $\pm$  SD,  $n = 10$ , Fig. 2). The calculated Nernst potential of  $K^+$  in the experimental solutions was  $-54$  mV and the Nernst potentials of the three other permeant ions in the solutions,  $Ca^{2+}$ ,  $H^+$  and  $Cl^-$  were, respectively,  $\geq 200$  mV (with internal  $[Ca^{2+}]$  buffered at  $<10^{-7}$  M),  $+100$  and  $-10$  mV. This confirms the previous determinations of the very high selectivity for  $K^+$  of the  $K_H$  channels in similar experimental conditions (Schroeder, 1988; Schroeder, 1995).

pH changes affected neither the reversal potential (Fig. 2B) nor the linearity of the instantaneous current-voltage curves. In contrast, the whole-cell steady-state  $K_H$  channel conductance,  $G_K$  (Eq. 1), increased with acidification (Figs. 2B and 3). Note that while between pH 8.1 and 5.5 the increase was below 30% at all membrane potentials, between 5.5 and 4.4  $G_K$  increased by 30–150% (depending on voltage) with acidification (Figs. 2B and 3).

#### THE EFFECT OF PROTONS ON THE STEADY-STATE PROPERTIES OF $G_K$

To learn how the steady-state activation of the  $K_H$  channel by hyperpolarization is altered by external protons, we fitted the steady-state  $G_K$ - $E_M$  relationships of each cell at the various pHs with the Boltzmann distribution (Eq. 4; see Materials and Methods). The averaged parameters (Table 1) then served to reproduce the “average”  $G_K$ - $E_M$  relationship at various pHs (Fig. 3: lines).

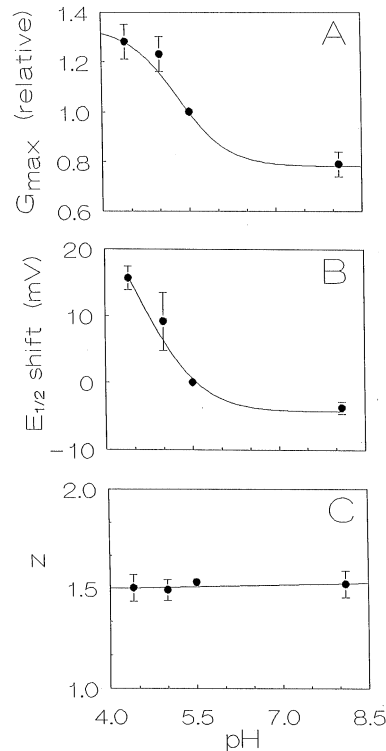


**Fig. 4.** pH dependence of the averaged parameters ( $\pm$ SEM) of individual steady state  $G_K$ - $E_m$  relationships (Table 1). (A)  $G_{max}$ , the maximum, voltage-independent conductance vs. pH. (normalized; see Materials and Methods). Line: Henderson-Hasselbalch relationship (Eq. 5; Materials and Methods), with best fit-parameters ( $\pm$ Estimated Error (EE);  $n = 63$ ):  $pK_a = 5.3 \pm 0.2$ ,  $G' = 0.6 \pm 0.7$  nS, and  $G_{basal} = 0.8 \pm 0.5$  nS ( $R' = 0.531$ ). (B) The shift of  $E_{1/2}$ , the mid-activation voltage of  $G_K$  at various pHs, relative to  $E_{1/2}$  at pH 5.5. Line: fit of a surface charge model (Eqs. 7 and 8; Materials and Methods), with best fit parameters ( $\pm$ EE;  $n = 56$ ):  $B = -35 \pm 16$  mV,  $d_i = 30 \pm 9$  Å, and  $pK_{sc} = 4.2 \pm 0.5$  ( $R' = 0.722$ ). (C)  $z$ , the effective charge moved between the closed and open states, vs. pH. Line: linear regression, with slope 0.006 ( $n = 63$ ). Average  $z$  at all pHs was  $1.5 \pm 0.2$  ( $\pm$ SD;  $n = 63$ ).

The voltage-independent maximum conductance,  $G_{max}$ , as well as the half-activation voltage,  $E_{1/2}$ , were both altered by external pH and increased with acidification (Fig. 4A and B).  $G_{max}$  values (normalized to  $G_{max}$  at pH 5.5; see Materials and Methods) could be related to pH by the Henderson-Hasselbalch equation (Eq. 5, Fig. 4A: line), with a  $pK_a$  of 5.3. Fitting the  $E_{1/2}$  shift, relative to pH 5.5, vs. pH with the modified Grahame equation (Eqs. 8 and 9, Fig. 4B), yielded the following properties of the putative negative charges at the external surface of the membrane in the vicinity of the  $K_H$  channel: the average charge separation,  $d_i = 30$  Å, the pH near the membrane at which half of the charges are protonated,  $pK_{sc} = 4.2$  (corresponding to bulk pH of 4.6) and the surface potential at pH 5.5,  $B = -35$  mV.

In contrast to the change in  $E_{1/2}$ , the average values of  $z$  at different pHs did not vary significantly (Fig. 4C)

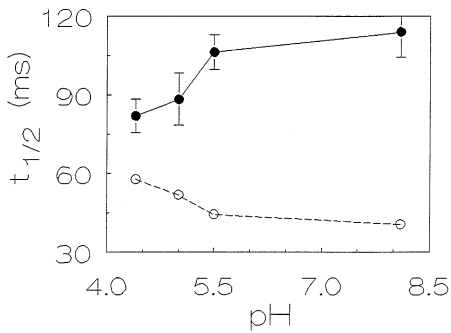


**Fig. 5.** The rate of activation increases and the rate of deactivation decreases with acidification (below pH 5.5). pH dependence of mean  $t_{1/2}$ , half time, ( $\pm$ SEM) of activation at  $-197$  mV (●) and of deactivation at  $-87$  mV (○). Where not visible, the error bars are smaller than the symbol size. Data from the cells of Fig. 3.

and their mean was 1.5 (This value of  $z$  is very similar to the value of 1.6 in the intact guard cell  $K_H$  channel [Blatt, 1992] and, not surprisingly, to the value of 1.7 we obtained by fitting the Boltzman relationship (Eq. 4) to the *Shaker*  $G_K/G_{max}$  vs.  $E_M$  data of Zagotta and Aldrich [1990]).

#### THE EFFECT OF pH ON $K_H$ CHANNEL KINETICS

Figure 5 depicts the dual effect of acidification below pH 5.5 on  $K_H$  channels kinetics: a decrease of the “half activation time” at  $-197$  mV (solid circles), and an increase of the “half deactivation time” at  $-87$  mV (open circles). The acceleration of activation and the retardation of deactivation are consistent with the enhancing effect of protons on  $K_H$  channel currents.

To gain more insight into the effects of pH on  $K_H$  channel gating, we chose to examine more closely the kinetics of macroscopic relaxations. Figure 6 illustrates the time course of activating (Fig. 6A) and deactivating (Fig. 6B) whole-cell  $K_H$  current from one cell fitted with three types of models for channel gating: (i) a two-state (C-O) model of a single gating unit; (ii) a two-identical-subunits model, in which each subunit independently undergoes C-O transitions, but both of them need to be in the O state for the channel to be open; (iii) a sequential three-state model of a single gating subunit. These data were best fitted with the three-state model (i.e., two exponentials). The delays, observed in both the activation and deactivation of currents, became more pronounced at a lower temperature ( $13^\circ\text{C}$ ; Ilan et al., 1995) indicating that they are not artifacts (*see also* Kourie & Goldsmith, 1992).

We fitted  $\tau$ s of activation and deactivation vs.  $E_M$  simultaneously with  $G_K-E_M$ , with the appropriate functions of the CCO model (Eqs. 10–13).

#### pH EFFECTS ON THE CCO MODEL PARAMETERS

The CCO model was fitted simultaneously to steady-state and kinetics data (*see* Materials and Methods) ex-

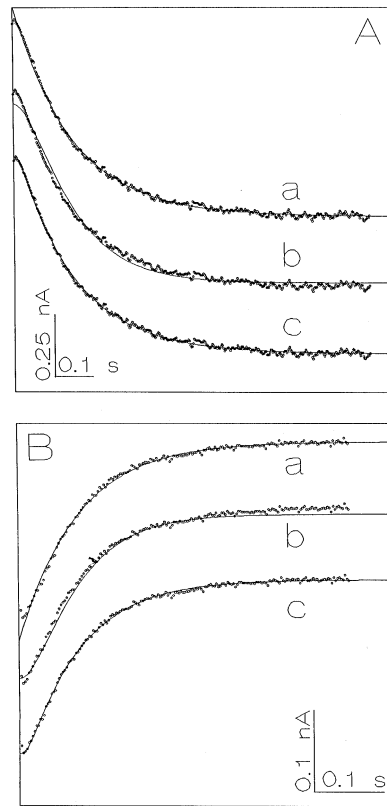


**Fig. 6.** A three-state model (C-C-O): the simplest necessary to fit macroscopic kinetics of gating. (A) Activation. Dotted traces: currents at a step from a holding potential of  $-87$  to  $-177$  mV, at pH 5.5. Lines: best fit to: (a) C-O model:  $A_o + A_1 e^{-t/\tau}$  ( $A_o = -845$  pA,  $A_1 = 850$  pA,  $\tau = 153$  msec,  $R' = 0.9982$ ); (b) classical Hodgkin-Huxley, two-identical- independent- C-O -subunits model:  $A_o + A_1[1 - e^{-t/\tau}]^2$  ( $A_o = -104$  pA,  $A_1 = -726$  pA,  $\tau = 100$  msec,  $R' = 0.9952$ ) and (c) C-C-O model:  $A_o + A_1 e^{-t/\tau_1} + A_2 e^{-t/\tau_2}$  ( $A_o = -843$  pA,  $A_1 = -93$  pA,  $A_2 = 887$  pA,  $\tau_1 = 8$  msec,  $\tau_2 = 148$  msec,  $R' = 0.9990$ ). (B) Deactivation. Dotted traces: currents at a step from a 2.5-sec pulse at  $-177$  to  $-87$  mV, at pH 5.5. Lines: best fit to: (a) C-O model:  $A_o + A_1 e^{-t/\tau}$  ( $A_o = -22$  pA,  $A_1 = -242$  pA,  $\tau = 77$  msec,  $R' = 0.9988$ ); (b) classical Hodgkin-Huxley, two-identical- independent- C-O -subunits model:  $A_o + A_1[1 - e^{-t/\tau}]^2$  ( $A_o = -227$  pA,  $A_1 = 200$  pA,  $\tau = 55$  msec,  $R' = 0.9980$ ) and (c) C-C-O model:  $A_o + A_1 e^{-t/\tau_1} + A_2 e^{-t/\tau_2}$  ( $A_o = -23$  pA,  $A_1 = 43$  pA,  $A_2 = -256$  pA,  $\tau_1 = 10$  msec,  $\tau_2 = 72$  msec,  $R' = 0.9993$ ).

tracted from experiments conducted at pH 5.5 (eight cells) and at pH 4.4 (four cells), between which protons affected gating. In an initial series of trials we found that the two parameters  $E_1$  and  $E_2$  did not differ significantly, and therefore we decided to use instead only one parameter,  $E_o$ . Table 2 summarizes the values of parameters obtained from the fit. Within the framework of the CCO model, changing pH from 5.5 to 4.4 shifted significantly, by 26 mV, the characteristic potential  $E_o$  while other parameters were not affected significantly. A similar shift, 25 mV, was observed also between  $E_{1/2}$  values obtained by fitting the same data with the simpler C-O

**Table 2.** The effect of pH on the parameters of the CCO model for  $K_H$  channels

pH	$E_o$	$z_\alpha$	$z_\beta$	$z_\gamma$	$z_\delta$	$B_1$ (sec <sup>-1</sup> )	$B_2$ (sec <sup>-1</sup> )	$z_1 + z_2$
5.5	$-137 \pm 6$	$0.39 \pm 0.18$	$0.60 \pm 0.07$	$0.26 \pm 0.14$	$0.42 \pm 0.15$	$42.7 \pm 5.9$	$4.05 \pm 0.59$	1.67
4.4	$-111 \pm 7$	$0.39 \pm 0.18$	$0.60 \pm 0.10$	$0.25 \pm 0.18$	$0.30 \pm 0.21$	$51.0 \pm 7.7$	$4.96 \pm 0.73$	1.54

$G_K$ - $E_M$  and  $\tau$ - $E_M$  relationships, pooled separately at pH 5.5 (8 cells) and pH 4.4 (4 cells), were fitted simultaneously with Eqs. 10–13. Listed are the best fit parameters ( $\pm 95\%$  confidence range). The “goodness of fit” indicator,  $R'$ , for the  $P_o$ - $E_M$ ,  $\tau_1$ - $E_M$  and  $\tau_2$ - $E_M$  data were for pH 5.5: 0.96, 0.09, 0.84, respectively and for pH 4.4: 0.96, 0.03, 0.88, respectively.

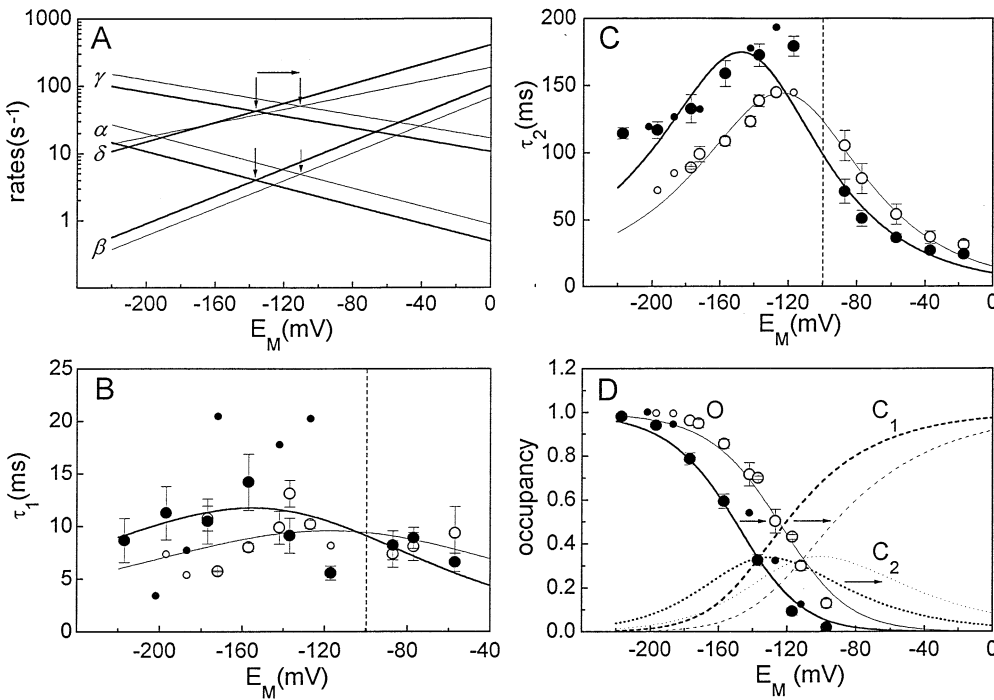


**Fig. 7.** Fitting the C-C-O model simultaneously to  $P_o$ - $E_M$ ,  $\tau_1$ - $E_M$  and  $\tau_2$ - $E_M$  relationships of the  $K_H$  channel at two pH values: 5.5: ●● and 4.4: ○○. Small symbols mark data from one individual experiment, large symbols represent mean of 4–8 experiments,  $\pm$ SEM. (Where not shown, errors were smaller than the symbol sign.) (A) voltage dependence of transition rate constants,  $\alpha$ ,  $\beta$ ,  $\gamma$ ,  $\delta$  (lines: Eqs. 10) at the two pHs: 5.5 (bold lines) and 4.4 (thin lines). Vertical arrows mark the characteristic voltages of the transitions between adjacent states,  $E_o$ , at both pHs. Horizontal arrow: the shift of  $E_o$  with acidification. (B)  $\tau_1$  vs.  $E_M$  (line: Eq. 11 with “+” before square root). Activation at the left and deactivation at the right of the vertical dashed line. Tail currents at  $-37$  and  $-17$  mV were fitted only with one exponential and the resulting  $\tau$  was included with the longer  $\tau$ s. (C)  $\tau_2$  vs.  $E_M$  (line: Eq. 11 with “-”). Activation at the left and deactivation at the right of the vertical dashed line. (D) The pH and voltage dependence of the calculated occupancies,  $P_o$ ,  $P_{C_1}$ ,  $P_{C_2}$  of the open, far-closed and middle-closed states  $O$ ,  $C_1$ ,  $C_2$ , respectively. Lines: solid:  $P_o$  of  $O$ : Eq. 12; dashed:  $P_{C_1}$  of  $C_1$ : Eq. 12 in which  $\alpha$  switched positions with  $\delta$ , and  $\beta$  with  $\gamma$ ; dotted:  $P_{C_2}$  of  $C_2$ :  $1 - (P_o + P_{C_1})$ . Best fit parameters are listed in Table 2.

model (Eq. 4). The larger shift in this subset of cells (compared to 11 mV in all of the cells; Table 1) may be related perhaps to the simpler kinetics of this subset (see Materials and Methods). The total number of effective charges moved between the extreme conformations was at least two, and was pH independent.

Figure 7 illustrates the fit of the model to the data at pH 5.5 and 4.4. Fig. 7A depicts the exponential dependence of the putative transition rate constants  $\alpha$ ,  $\beta$ ,  $\gamma$  and  $\delta$  on membrane potential at these pH values. The char-

acteristic voltage  $E_o$  shifted by 26 mV (Table 2) between pH 5.5 and 4.4. These rate constants were used to re-construct the fit to the data in Fig. 7B–D. Figure 7B and C depict the effect of pH change from 5.5 to 4.4 on the  $\tau$ s of activation and deactivation. Acidification diminished the value of peak  $\tau_2$  by about 15% (Fig. 7C). Nevertheless, both pairs of  $\tau$ - $E_M$  curves still cross over. Thus, the shifts of the  $\tau$ s in the depolarizing direction with acidification explain the opposite effects of pH on  $t_{1/2}$  at  $-197$  mV and  $t_{1/2}$  at  $-87$  mV (Fig. 5). Figure 7D



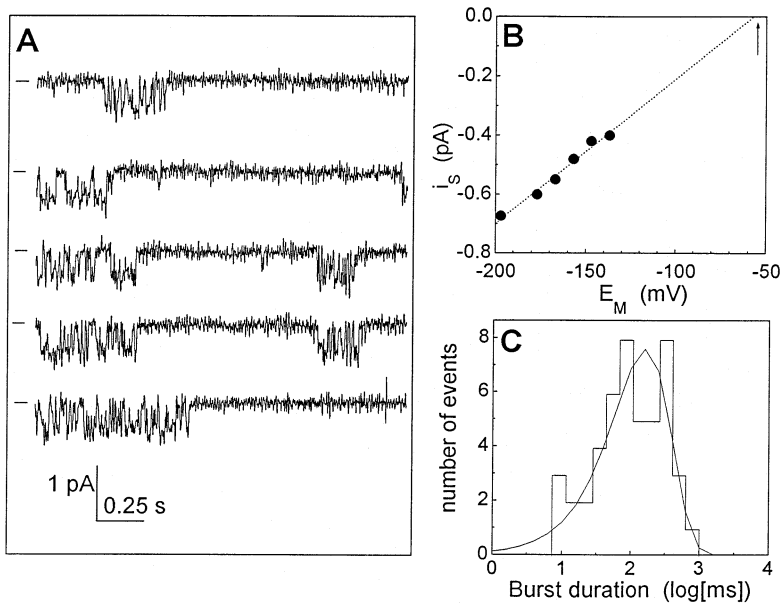


**Fig. 8.**  $K_H$  channels open in bursts. (A) Sample single-channel records from an outside-out patch at a constant hyperpolarization to  $-167$  mV. Dashes at the left indicate the closed-channel current level. Filter: 100 Hz. (B) Current-voltage relationship of an open channel at pH 5.5. Dotted line: linear regression to data points. The unitary conductance was  $4.9 \pm 0.3$  pS, and the reversal potential was  $-57$  mV (with the lower and upper fiducial limits of  $-76$  and  $-32$  mV, respectively). Arrow:  $E_K$ , the calculated  $K^+$  Nernst potential. (C) Burst duration histogram (see Materials and Methods). Line: exponential fit to the data. The mean burst duration was 161 msec.

illustrates the distribution of the  $K_H$  channels between the three states at pH 4.4 and 5.5. The fit of the CCO model to the data (solid lines) reconstructs the observed shift of  $P_o$  (symbols) in the depolarized direction as pH decreases from 5.5 to 4.4. The calculated occupancies of states  $C_1$  and  $C_2$  (dashed and dotted lines) shift similarly.

In support for our model derived from the whole-cell data, we found that the average burst duration of single channels in one experiment in similar conditions, at pH 5.5 and  $-167$  mV (Fig. 8A), was 161 msec (Fig. 8C), corresponding to rate of “burst closure” of  $\sim 6 \text{ sec}^{-1}$ , similar to the estimate of  $\beta$  at this potential (Fig. 7A). These channels were identified by their reversal potential close to  $E_K$  (Fig. 8B) and their voltage dependence (*not shown*). It has been suggested that these bursts represent the  $K_H$  channel openings, and the flicker—the block of the open channel by a permeating ion (Schroeder et al., 1994; *see also* Discussion).

## Discussion

### THE CCO MODEL DESCRIPTION OF $K_H$ CHANNELS IN *V. faba*

This paper is the first attempt to describe the gating of the protoplast *native*  $K_H$  channel with a model reproducing the sigmoidal time course of the inward K currents. While Fairley-Grenot and Assmann (1993) fitted the macroscopic  $K_H$  currents from *V. faba* as well as from *Zea mays* protoplasts with a single exponential (two-state model), the delay in activation in *Avena sativa* protoplasts was fitted by two exponentials (Kourie & Goldsmith, 1992). The delay in activation of the cloned

$K_H$  channel (KAT1) was accounted for by a power function (Hoshi, 1995) like the classical HH model (Hodgkin & Huxley, 1952) for independent 2-state-subunits. In the present work we fitted the  $K_H$  channel currents, in a subpopulation of *V. faba* guard-cell protoplasts, by two exponentials and formulated a sequential three state model (CCO: Closed-Closed-Open) describing the kinetics and the steady-state gating of these channels in the range of roughly 5–500 msec<sup>3</sup>. Mathematically, the HH model with two subunits is equivalent to a CCO model with particularly constrained rate constant values and only four parameters (Armstrong, 1969), while we used a CCO model with seven parameters. Although our model fitted well the macroscopic currents (Fig. 6), this is still a reduced model, since in the single channel records the channel openings appeared in bursts (Fig. 8). It is likely, that the fast “flicker” of open channels results not from submillisecond conformational transitions but from blocking of ion passage through the open channel by various ions, as suggested for the K channels of *Saccharomyces cerevisiae* (Bertl, Slayman & Gradmann, 1993) or the *Shaker* channels (Hoshi, Zagotta & Aldrich, 1994). This ion could be  $\text{Ca}^{2+}$ , which can access the  $K_H$  channel (Fairley-Grenot & Assmann, 1992). If, in this reduced model, the O state represents lumped Open  $\leftrightarrow$  Blocked transitions, the rate constant  $\beta$  should predict the inverse of average burst duration. Indeed, in support for this model, the mean burst duration in this single-channel experiment (Fig. 8C) was predictable from the macroscopic data (Fig. 7A).

<sup>3</sup> Fitting the currents in the other subpopulation of cells required an additional longer time constants, e.g., of about 1 sec at  $-160$  mV.

According to the CCO model, all of the transitions are voltage sensitive. There are no other results from this type of analysis of plant  $K_H$  channels available for comparison. We can only compare the more general description of kinetics of  $K_H$  current activation and deactivation. In this work, the longer  $\tau$  of  $K^+$  current activation ( $\tau_2$ ) was voltage dependent similarly to that of the deactivation (Fig. 7C). A similar conclusion can be drawn from the comparison of  $t_{1/2}$  of activation to  $\tau$  of deactivation of the  $K_H$  current in the intact guard cells (Blatt, 1992). In contrast, others find that  $\tau$  and  $t_{1/2}$  of activation of the protoplasts  $K_H$  channels is voltage independent while emphasizing the strong voltage dependence of the deactivation kinetics of  $K_H$  channels in protoplasts (Fairley-Grenot & Assman, 1993; Schroeder, 1995) and the KAT1 clone in *Xenopus* (Hoshi, 1995).

#### THE MECHANISM OF pH EFFECT

The results presented above constitute the first description of the effects of external protons on the native  $K_H$  channel in protoplasts. The range of external pH examined in this work (4.4–8.1) exceeds that in all other reports on both native and cloned plant channels (Blatt, 1992; Hoshi, 1995; Hedrich et al., 1995; Muller-Rober et al., 1995; Véry et al., 1995).

In *V. faba* protoplasts, extracellular protons (pH between 8.1 and 4.4) exert a significant enhancing effect on the macroscopic conductance of the  $K_H$  channel. We ascribe these effects of protons solely to the *external* surface of the membrane, due to the efficient buffering of the internal solution (Marty & Neher, 1983). To resolve which of the two factors making up the macroscopic conductance, the voltage-dependent  $P_o$ , or the voltage-independent  $G_{\max}$ , are responsible for these external protons effects, we examined each one separately.

#### pH EFFECTS ON THE VOLTAGE-INDEPENDENT $G_{\max}$

The lack of pH effect on the reversal potential of the  $K_H$  currents, even with over three orders of magnitude increase of external proton concentration from pH 8.1 to 4.4, is predictable from a calculation using the Goldman-Hodgkin-Katz voltage equation taking into account the small concentration of  $H^+$  and assuming that the permeability for  $H^+$  does not exceed that for  $K^+$ . Based on this assumption, it is very unlikely that protons would contribute directly to the increase of the single channel's conductance. If anything, by screening negative charges in the channel vicinity and, consequently, decreasing the concentration of  $K^+$  near the channel mouth, protons might be expected to *decrease* the unitary conductance (as in Zhang & Siegelbaum, 1991). In at least one rare case, where external protons increased the macroscopic conductance, single-channel

conductance was not affected (Hanke & Miller, 1983). Consequently, the increase in the voltage-independent maximum  $K_H$  conductance ( $G_{\max}$ ) ought to be attributed to the number of available channels,  $N$  (Eq. 6).

#### *A Low-affinity Site in the Protoplast and in the KAT1 Clone Expressed in an Oocyte?*

In view of the fast reversibility of the pH effects (on the order of a few minutes) it is unlikely that the total number of channels in the cell membrane varies. Rather, it may be concluded that protons affect the voltage-independent fraction of the available channels in the membrane,  $f_a$  (Eq. 7). We may speculate that protonation of a "site" (or a class of sites) with an apparent  $pK_a$  of 5.3 "unlocks" additional channels rendering them able to change their conformation in response to changes in the membrane electrical field. Such value of  $pK_a$  is characteristic of a  $\beta$  or  $\gamma$  carboxyl group of an aspartic or glutamic acid in a nonpolar environment (Segel, 1975). The same site may be involved in pH sensing in the  $K_H$  channel clone KAT1 expressed in an oocyte, where an external pH change from 6.5 to 5.0 increased  $G_{\max}$  (current scaling factor) by 40% (Véry et al., 1995), similarly to protoplasts at this pH range (Fig. 4A).

#### *A High-affinity Site in the Intact Guard Cell*

In intact *V. faba* guard cells (Blatt, 1992) external pH effects were examined only between 5.5 and 8.1. At pH 5.5 the maximum  $K_H$  specific conductance of the intact guard cell ( $\sim 0.3$  mS/cm<sup>2</sup>; Blatt, 1992) is comparable to that of the protoplast ( $\sim 0.6$  mS/cm<sup>2</sup>; see Materials and Methods and Table 1). At pH 8.1, however, the specific conductance of the guard cell is 20-fold smaller than that of the protoplast. Thus in the intact guard cells alkalization from pH 5.5 to 8.1 decreased the  $G_{\max}$  values over 10-fold (Blatt, 1992), while in the isolated protoplasts we observed only a roughly 20% decrease of  $G_{\max}$  at this pH range. This striking diminution of  $G_{\max}$  in the intact guard cells may be due to an additional site (on the  $K_H$  channel itself or in its vicinity) in the intact guard cell (but not in the protoplast), which, upon deprotonation "locks" the channel gates in a nonconducting conformation. Indeed, fitting Eq. 5 to the  $G_{\max}$  vs. pH data from the intact guard cell (data from Fig. 10 of Blatt, 1992) yielded an apparent  $pK_a$  of  $7.2 \pm 0.09$  ( $\pm EE$ ). Based on this  $pK_a$  value, possible candidates for this putative site in the intact guard cells could be an imidazolium of a histidine in a nonpolar environment, or an  $\alpha$  amino group or a sulfhydryl group of a cysteine (Segel, 1975).

#### pH EFFECTS ON THE VOLTAGE-DEPENDENT GATING: NEGATIVE SURFACE CHARGE NEAR THE $K_H$ CHANNEL

In addition to the above "enabling" effect through one or two sites located on the channel or in its vicinity,

protons affect directly the voltage-dependent gating of the  $K_H$  channel. This is evident from the following responses of native  $K_H$  channels to external acidification: (i) A positive shift of  $P_o$ - $E_M$  relationship, quantified as the shift in the half-saturation point, both in intact guard cells (Blatt, 1992) and in protoplasts (this work); (ii) acceleration and the slowing down of currents during activation and deactivation, respectively, in the guard cells (Blatt, 1992) and in protoplasts (this work). The change in the kinetics ( $\tau$ s) appears also to reflect a shift along the voltage axis, in a direction similar to that of  $P_o$  (Figs. 4B, 7B–7D). Acceleration of activating  $K_H$  currents kinetics with acidification (pH 7.4–4.5) has been noted also for the  $K_H$  channel clone from a potato guard-cell expressed in oocytes, KST1 (Muller-Rober et al., 1995). There are two reports concerning proton effects on gating of the *Arabidopsis*  $K_H$  channel clone, KAT1. In the clone, like in the protoplast  $K_H$  channel, Hedrich et al. (1995) reported also acceleration and the slowing down of currents during activation and deactivation, respectively, and found a significant positive shift, of  $\sim 20$  mV, by protons of the steady-state half activation potential between pH 5.5 and 4.5. Véry et al., (1995) did not observe any KAT1 gating dependence on external pH in the 7.5–5.0 range. We suggest, however, that they could have observed such effects had they lowered the pH further.

We interpret these effects of protons on gating as the modification of the electrical field sensed by the gates. The mechanism of this modification is the decrease, by protons, of the negative surface charge density at the external surface of the membrane. This surface charge effect need not stem from a homogenous spread of negative charges on the membrane. Rather, it may be confined to the vicinity of the channel gates. We have modeled this effect as due to both nonspecific charge screening and binding to the negative charges (Gilbert & Ehrenstein, 1969, 1970). The effect of external surface charges on  $K_H$  channel gating in an intact guard cell has been already implicated in the shift of open probability by increased external  $Ca^{2+}$  concentration (Blatt, 1992; we suggest that the lack of effect of increased external  $K^+$  concentration in that report may be due to the presence of a relatively high  $Ca^{2+}$  concentration (5 mM) in those experiments).

#### *A Low-affinity Site in the Protoplast and in the KAT1 Clone Expressed in an Oocyte?*

Out of the seven parameters of the CCO model, only one,  $E_o$ , was affected by protons between pH 5.5 and 4.4 (Table 2). The increase of  $E_o$  suggests, as in the two-state gating model, that protonation increases the electrical field in the membrane. Based on a two-state model for the  $K_H$  channel gating and a model for a surface

charge effect, the results appear consistent with a titration of surface charges, with  $pK_{sc}$  of 4.2 at the membrane equivalent to an apparent (bulk)  $pK_{sc}$  of 4.6. Although the membranes of guard-cell protoplast and the oocyte are probably rather different, the shift of  $P_o$  and the accelerated activation occurred at the same pH range in the protoplast  $K_H$  channel (this work) and the KAT1 clone (Hedrich et al., 1995). This similarity suggests that the low-affinity protonation site (negative surface charge) resides on part of the channel itself. This conclusion is supported by the dissimilarity of the corresponding site related to the  $K_D$  channel that coexists with the  $K_H$  channel in the same plasma membrane. This site of the  $K_D$  channel was protonated with an apparent  $pK_{sc}$  of 5.0 (Ilan et al., 1994a).

The candidate residues with such negative charges in the  $K_H$  channel (apparent  $pK_{sc}$  of 4.6) might be a  $\beta$  or  $\gamma$  carboxyl of an aspartic or glutamic acid (Segel, 1975). Glutamate and aspartate residues, found in the S4-S5 linker of the plant  $K_H$  channel molecule (at positions 186 and 188, respectively), are conserved among the various clones of this channel (Cao, Crawford & Schroeder, 1995). It is tempting to speculate that since the S4-S5 linker is presumably part of the pore lining (at the internal vestibule; reviewed by Kukuljan, Labarca & Latorre, 1995), one or both of these residues can be reached by the external protons. Since the S4-S5 linker is also implicated in the modulation of gating (Kukuljan et al., 1995), protons may affect gating via one of these residues. Consequently, these residues might be identified with the titratable negative surface charges.

#### *A High-affinity Site in the Intact Guard Cell?*

In the intact guard cell, acidification between pH 8.1 and 5.5 induced shifts of  $E_{1/2}$  (Blatt, 1992). We fitted these shifts (Fig. 10 of Blatt, 1992) with the surface charge model (Eqs. 8 and 9) and obtained a  $pK_{sc}$  of 6.4 ( $\pm 0.1$ ) at the membrane, equivalent to an apparent  $pK_{sc}$  of 7.1, characteristic of an imidazolium group of a histidine (Segel, 1975). These pronounced voltage shifts of  $E_{1/2}$  (Blatt, 1992) contrast with the lack of significant effect in the same range of pH in protoplasts (Fig. 4B) and in the KAT1 clone (Véry et al., 1995; Hedrich et al., 1995). Just as in the former case (the high-affinity protonation site affecting  $G_{max}$  in the intact guard cell vs. protoplasts), this discrepancy may be attributed to the existence of a high-affinity protonation site in the intact guard cell. This site appears to be missing from the native channel in the protoplast and from the KAT1 channel in the oocyte. Consequently, it might be located in the membrane in the vicinity of the  $K_H$  channel and might not constitute a part of the channel itself. It should be noted that these values of  $pK_a$  obtained for the intact cell in Blatt's experiments might be somewhat inaccu-

rate, owing to the buffering effect of the cell wall, pronounced most in the vicinity of the relatively low “bulk  $pK_a$ ” of roughly four (Saftner & Rashke, 1981).

## PHYSIOLOGICAL SIGNIFICANCE

The modulatory effects of pH on  $K_H$  channels are consistent with the physiological requirements for their function. At the apoplastic pH of  $\sim 5$ , prevailing when the stomatal guard cells swell and stomata open (Edwards et al., 1988), acidification will not interfere with the opening of the  $K_H$  channels by hyperpolarization. On the contrary, acidification might even enhance  $K_H$  influx. Indeed, a possible concomitant increase in proton-coupled solute influx through carriers, as well as the influx of  $K^+$  ions themselves through the  $K_H$  channels, would tend to depolarize the membrane (Ullrich & Novacky, 1990). Additionally, some incidental signals might bring about depolarization by an increase in permeability to  $Ca^{2+}$  or to  $Cl^-$ . This would result in a decreased driving force for  $K^+$ . However, since net  $K^+$  influx depends both on the driving force for  $K^+$  as well as on  $G_K$  (Eq. 1), the increase in  $K_H$  membrane conductance brought about by external acidification would compensate for the loss of the driving force and might even exceed it.

Thanks are due to Ms. A. Ben David for help in protoplast isolation, to Dr. E. Schachtman for help with the statistics and to Dr. H. Jarosch for help with the SAS and the Fortran fitting routines.

This research was supported by the Israel Science Foundation grant administered by the Israel Academy of Sciences and Humanities grant No. 454/93 to AS and by grants from the US-Israel Binational Foundation (No. 91-00293) and from the US-Israel Binational Agricultural Research and Development (No. IS-2469-94RC) to NM.

## References

- Anderson, J.A., Huprikar, S.S., Kochian, L.V., Lucas, W.J., Gaber, R.F. 1992. Functional expression of a probable *Arabidopsis thaliana* potassium channel in *Saccharomyces cerevisiae*. *Proc. Natl. Acad. Sci. USA* **89**:3736–3740
- Armstrong, C.M. 1969. Inactivation of the potassium conductance and related phenomena caused by quaternary ammonium ion injection in squid axons. *J. Gen. Physiol.* **54**:553–575
- Assmann, S.M., Simoncini, L., Schroeder, J.I. 1985. Blue light activates electrogenic ion pumping in guard cell protoplasts of *Vicia faba*. *Nature* **318**:285–287
- Behrens, M.I., Oberhauser, A., Bezanilla, F., Latorre, R. 1989. Batrachotoxin-modified sodium channels from squid optic nerve in planar bilayers. *J. Gen. Physiol.* **93**:23–41
- Bertl, A., Slayman, C.L., Gradmann, D. 1993. Gating and conductance in an outward-rectifying  $K^+$  channel from the plasma membrane of *Saccharomyces cerevisiae*. *J. Membrane Biol.* **132**:183–199
- Blatt, M.R. 1992.  $K^+$  channels of stomatal guard cells: characteristics of the inward rectifier and its control by pH. *J. Gen. Physiol.* **99**:615–644
- Blum, D.E., Elzenga, J.T.M., Linnemeyer, P.A., Van Volkenburgh, E. 1992. Stimulation of growth and ion uptake in bean leaves by red and blue light. *Plant Physiol.* **100**:1968–1975
- Bowling, D.J.F. 1987. Measurement of the apoplastic activity of  $K^+$  and  $Cl^-$  in the leaf epidermis of *Commelina communis* in relation to stomatal activity. *J. Exp. Bot.* **38**:1351–1355
- Cao, Y., Crawford, N.M., Schroeder, J.I. 1995. Amino terminus and the first four membrane-spanning segments of the Arabidopsis  $K^+$  channel KAT1 confer inward-rectification property of plant-animal chimeric channels. *J. Biol. Chem.* **270**:17697–17701
- Edwards, M.C., Smith, G.N., Bowling, D.J.F. 1988. Guard cells extrude protons prior to stomatal opening—A study using fluorescence microscopy and pH micro-electrode. *J. Exp. Bot.* **39**:1541–1547
- Ehrenstein, G., Blumenthal, R., Latorre, R., Lecar, H. 1974. Kinetics of the opening and closing of individual excitability-inducing material channels in a lipid bilayer. *J. Gen. Physiol.* **63**:707–721
- Fairley-Grenot, K.A., Assmann, S.M. 1992. Permeation of  $Ca^{2+}$  through  $K^+$  channels in the plasma membrane of *Vicia faba* guard cells. *J. Membrane Biol.* **128**:103–113
- Fairley-Grenot, K.A., Assmann, S.M. 1993. Comparison of  $K^+$ -channel activation and deactivation in guard cells from a dicotyledon (*Vicia faba* L.) and a graminaceous monocotyledon (*Zea mays*). *Planta* **189**:410–419
- Gilbert, D.L., Ehrenstein, G. 1969. Effect of divalent cations on potassium conductance of squid axons: Determination of surface charge. *Biophys. J.* **9**:447–463
- Gilbert, D.L., Ehrenstein, G. 1970. Use of a fixed charge model to determine the pK of the negative sites on the external membrane surface. *J. Gen. Physiol.* **55**:822–825
- Grahame, D.C. 1947. The electrical double layer and the theory of electrocapillarity. *Chemical Reviews* **41**:441–501
- Hamill, O.P., Marty, A., Neher, E., Sakmann, B., Sigworth, F. 1981. Improved patch-clamp techniques for high-resolution current recording from cells and cell-free membrane patches. *Pfluegers Arch.* **391**:85–100
- Hanke, W., Miller, C. 1983. Single chloride channels from *Torpedo* electroplax; Activation by protons. *J. Gen. Physiol.* **82**:25–45
- Hedrich, R., Moran, O., Conti, F., Busch, H., Becker, D., Gambale, F., Dreyer, I., Kuch, A., Neuwinger, K., Palme, K. 1995. Inward rectifier potassium channels in plants differ from their animal counterparts in response to voltage and channel modulators. *Eur. Biophys. J.* **24**:107–115
- Hedrich, R., Schroeder, J.I. 1989. The physiology of ion channels and electrogenic pumps in higher plants. *Ann. Rev. Plant Physiol.* **40**:539–569
- Hodgkin, A.I., Huxley, A.F. 1952. A quantitative description of membrane current and its application to conduction and excitation in nerve. *J. Physiol.* **117**:500–544
- Hoshi, T. 1995. Regulation of voltage dependence of the KAT1 channel by intracellular factors. *J. Gen. Physiol.* **105**:309–328
- Hoshi, T., Zagotta, W.N., Aldrich, R.W. 1994. *Shaker* potassium channel gating I: transitions near the open state. *J. Gen. Physiol.* **103**:249–278
- Huang, L.Y.M., Moran, N., Ehrenstein, G. 1984. Gating kinetics of batrachotoxin-modified sodium channels in neuroblastoma cells determined from single-channel measurements. *Biophys. J.* **45**:313–322
- Ilan, N., Moran, N., Schwartz, A. 1995. The role of potassium channels in the temperature control of stomatal aperture. *Plant Physiol.* **108**:1161–1170
- Ilan, N., Schwartz, A., Moran, N. 1994a. External pH effects on the depolarization-activated K channels in guard cell protoplasts of *Vicia faba*. *J. Gen. Physiol.* **103**:807–831
- Ilan, N., Schwartz, A., Moran, N. 1994b. Protons enhance the hyper-

- polarization-activated K channel in the plasma membrane of *Vicia faba* guard cell protoplasts. *Plant Physiol.* **S105**:144
- Ilan, N., Schwartz, A., Moran, N. 1996. External protons enhance the inward-rectifying K channel in plant stomatal guard cell protoplast. *Biophys. J.* **70**:400a. (Abstr.)
- Ketchum, K.A., Slayman, C.W. 1996. Isolation of an ion channel gene from *Arabidopsis thaliana* using the H5 signature sequence from voltage-dependent  $K^+$  channels. *FEBS Lett.* **378**:19–26
- Kourie, J., Goldsmith, M.H.M. 1992.  $K^+$  channels are responsible for an inwardly rectifying current in the plasma membrane of mesophyll protoplasts of *Avena sativa*. *Plant Physiol.* **98**:1087–1097
- Kukuljan, M., Labarca, P., Latorre, R. 1995. Molecular determination of ion conduction and inactivation in  $K^+$  channels. *Am. J. Physiol.* **268**:C535–C556
- Lee, Y., Satter, R.L. 1989. Effects of white, blue, red light and darkness on pH of the apoplast in *Samanea pulvinus*. *Planta* **178**:31–40
- Lowen, C.Z., Satter, R.L. 1989. Light-promoted changes in apoplastic  $K^+$  activity in the *Samanea saman* pulvinus, monitored with liquid membrane microelectrodes. *Planta* **179**:421–427
- Marrè, E., Lado, P., Rasi-Cadogno, F., Colombo, R., De Michelis, M.I. 1974. Evidence for the coupling of proton extrusion to  $K^+$  uptake in Pea internode segments treated in fusicoccin or auxin. *Plant Science Lett.* **3**:365–379
- Marty, A., Neher, E. 1983. Tight seal whole-cell recording. In: Single Channel Recording. Sakmann B. and Neher E., Editors. Plenum Press, New York
- Muller-Rober, B., Ellenberg, J., Provart, N., Willmitzer, L., Busch, H., Becker, D., Dietrich, P., Hoth, S., Hedrich, R. 1995. Cloning and electrophysiological analysis of KST1, an inward rectifying  $K^+$  channel expressed in potato guard cells. *EMBO J.* **14**:2409–2416
- Neher, E. 1992. Correction for liquid junction potentials in patch-clamp experiments. *Methods Enzymol.* **207**:123–131
- Raschke, K., Humble, G.D. 1973. No uptake of anions required by opening stomata of *Vicia faba*: Guard cells release hydrogen ions. *Planta* **115**:47–57
- Robinson, R.A., Stokes, R.H. 1965. Electrolyte Solutions. Butterworths, London
- Saftner, R.A., Raschke, K. 1981. Electrical potentials in stomatal complexes. *Plant Physiol.* **67**:1124–1132
- Schroeder, J.I. 1988. Potassium transport properties of potassium channels in the plasma membrane of *Vicia faba* guard cells. *J. Gen. Physiol.* **92**:667–683
- Schroeder, J.I. 1995. Magnesium-independent activation of inward-rectifying  $K^+$  channels in *Vicia faba* guard cells. *FEBS Lett.* **363**:157–160
- Schroeder, J.I., Raschke, K., Neher, E. 1987. Voltage dependence of  $K^+$  channels in guard cell protoplasts. *Proc. Natl. Acad. Sci. USA* **84**:4108–4112
- Schroeder, J.I., Ward, J.M., Gassmann, W. 1994. Perspectives on the physiology and structure of inward-rectifying  $K^+$  channels in higher plants: biophysical implications for  $K^+$  uptake. *Ann. Rev. Biophys. Biomol. Struct.* **23**:441–471
- Segel, I.H. 1975. Effects of pH and temperature. In: Enzyme Kinetics. Behavior and Analysis of Rapid Equilibrium and Steady-State Enzyme Systems. pp. 884–926. John Wiley & Sons, New York
- Sentenac, H., Bonneaud, N., Minet, M., Lacroute, F., Salmon, J.-M., Gaymard, F., Grignon, C. 1992. Cloning and expression in yeast of a plant potassium ion transport system. *Science* **256**:663–665
- Shimazaki, K., Iino, M., Zeiger, E. 1986. Blue light-dependent proton extrusion by guard-cell protoplasts of *Vicia faba*. *Nature* **319**:324–326
- Sigworth, F.J. 1995. Voltage gating of ion channels. *Quart. Rev. Biophys.* **27**:1–40
- Sokal, R.R., Rohlf, F.J. 1981. Linear regression. In: Biometry. pp. 496–498. WH Freeman, New York
- Spanswick, R.M. 1981. Electrogenic ion pumps. *Ann. Rev. Plant Physiol.* **32**:267–289
- Starrach, N., Mayer, W.-E. 1989. Changes of the apoplastic pH and  $K^+$  concentration in the *Phaseolus pulvinus in situ* in relation to rhythmic leaf movements. *J. Exp. Bot.* **40**:865–873
- Ullrich, C.I., Novacky, A.J. 1990. Extra- and intracellular pH and membrane potential changes induced by  $K^+$ ,  $Cl^-$ ,  $H_2PO_4^-$ , and  $NO_3^-$  uptake and fusicoccin in root hairs of *Limnobium stoloniferum*. *Plant Physiol.* **94**:1561–1567
- Véry, A., Gaymard, F., Bosseux, C., Sentenac, H., Thibaud, J. 1995. Expression of a cloned plant  $K^+$  channel in *Xenopus* oocytes: analysis of macroscopic currents. *The Plant J.* **7**:321–332
- Zagotta, W.N., Aldrich, R.W. 1990. Voltage-dependent gating of Shaker A-type potassium channels in *Drosophila* muscle. *J. Gen. Physiol.* **95**:29–60
- Zeiger, E. 1983. The biology of stomatal guard cells. *Ann. Rev. Plant Physiol.* **34**:441–475
- Zhang, J.F., Siegelbaum, S.A. 1991. Effects of external protons on single cardiac sodium channels from guinea pig ventricular myocytes. *J. Gen. Physiol.* **98**:1065–1083